Synthesis, Characterization, Thermal Analysis and Structural Studies of New Complexes with Tetradentate Ligand

*Abbas A. Salih Al-Hamdani** *Sahar S. Hassan**

Received 13, May, 2014
Accepted 30, June, 2014

Abstract:

Some new complexes of 4-(5-(1,5-dimethyl-3-oxo-2-phenyl pyrazolidin-4-ylimino)-3,3-dimethyl cyclohexylideneamino) -1,5- dimethyl-2- phenyl -1H- pyrazol -3(2H) –one (L) with Mn(II), Fe(III), Co(II), Ni(II), Cu(II), Pd(II), Re(V) and Pt(IV) were prepared. The ligand and its metal complexes were characterized by phisco-chemical spectroscopic techniques. The spectral data were suggested that the (L) as a neutral tetradentate ligand is coordinated with the metal ions through two nitrogen and two oxygen atoms. These studies revealed Octahedral geometries for all metal complexes, except square planar for Pd(II) complex. Moreover, the thermodynamic activation parameters, such as ΔE^*, ΔH, ΔS, ΔG and K are calculated from the TGA curves using Coats –Redfern method. Hyper Chem -8 program has been used to predict structural geometries for compounds in gas phase. The heat of formation (ΔH_f) and bin ding energy (ΔE_b) at 298 °K for the free ligand and its metal complexes were calculated by PM3 method. The synthesized ligands and their metal complexes were screened for their biological activity against bacterial species, two Gram positive bacteria *(Bacillus subtilis and Staphylococcus aureus)* and two Gram negative bacteria (*Escherichia coli and Pseudomonas aeruginosa*).

Key words: Tetradentate ligand Schiff base; thermal analysis and Kinetics thermodynamic parameters.

Introduction:

The coordination chemistry of transition metals with ligands from the 5, 5- dimethyl cyclohexane-1,3- dione has been of interest due to different bonding modes show by these ligands with both electron rich and electron poor metals. Schiff bases play an important role in inorganic chemistry as they easily form stable complexes with most transition metal ions. The presence of donor atoms in the ligand will play in important role in the formation of a stable chelatering and this situation facilitates the complexation process[1]. Moreover, the synthesis, spectroscopic characterization and reaction of transition metal with hydrazine ligands have shown wide spectro of biological and pharmaceutical activates such as possess antimicrobial, antibacterial, antifungal, anti- inflammatory, anticonvulsant, antitubercular, antiviral, antioxidative effects and inhibition of tumor growth[2-4]. The aim of this paper is to synthesized, characterization, study thermal analysis and study the biological activates of the new complexes with tetradentate Schiff base ligand.

*Department of Chemistry, College of Science for Women, University of Baghdad, Iraq
Email: - Abbas_alhamadani@ yahoo. co. uK

Materials and Methods:

All reagents were commercially available and used without further purification. Solvent were distilled from appropriate drying agents immediately prior to use.

Infrared spectra were obtained using CsI discs (4000-200 cm^{-1}) on Perkin –Elmer FT-IR spectrometer. The electronic spectra were carried out using a Cary 50 Conc. UV-Visible spectra were recorded using spectrophotometer in DMSO solution 10^{-3} M. Thermal analysis studies of the complexes were performed on Perkin – Elmer pyris Diamond DTA / TG Thermal system under nitrogen atmosphere at a heating rate at 10ºC / min from 30-900 ºC. Elemental analysis (C, H, N) were performed by using a flash E A 1112 Series elemental analyzer. Chloride was determined using potentiometer titration method on a 686-Titro processor – 665 Dosimat Metrohm Swiss. Conductivity measurements were made with DMSO solution using a Jenway 4071 digital conductivity meter and room temperature. Magnetic moments were measured with a magnetic susceptibility balance (Jonson Mattey Catalytic system Division). Mass spectra were obtained by LC-Mass 100P Shimadzu. NMR spectra (^{1}H-, ^{13}C- NMR) were acquired in DMSO -d_6 solution using Brucker AMX 400 MHz spectrometer with tetramethyl silane (TMS) as an internal standard for ^{1}H NMR analysis. Metals were determined using a Shimadzu (A. A) 680 G atomic absorption spectrophotometer. Melting points were obtained on a Buchi SMP - 20capillary melting point apparatus and are uncorrected.

Preparation of the ligand:

To a solution of 5,5-dimethylcyclohexane- 1,3- dione (A) (1g,7.142 mmole) in ethanol (10ml), (5) drops of glacial acetic acid were added slowly, then the mixture was added to 4 –amino antipyrine (B) (2.905 g, 14.280 mmole) in ethanol (10 ml). The mixture was refluxed for (4hrs), with stirring at temperature (40 - 50 ºc) in water path. The deep yellow solution was left to dry for (24hrs) at room temperature. The obtained the precipitate was washed with an excess of mixture of ethanol and water (1:1), dried then drops of diethylether were added to precipitate which was dated in a crucible for (1min) with continuous stirring. After that the product precipitated yield (87%), m. p. (219-220ºc). The LC-Mass for ligand (510m/ z) with ($C_{30}H_{34}N_6O_2$), (327 m/ z) with ($C_{18}H_{23}N_4O_2$) and (326 m/ z) with ($C_{18}H_{22}N_4O_2$). ^{1}H-NMR (DMSO-d_6, ppm): δ 1.09 (s,6H, CCH_3), 1.69 (s,2H, CH), 1.73 (s,H,CH), 2.74 (s,6H,CCH_3), 3.43 (s,6H, NCH_3),7.13-8.03 (m,10H arom). ^{13}C-NMR (100.622 MHz, DMSO-d_6): δ 16.39 (C_{18}), 21.87 (C_5), 29.79 (C_1), 46.79 (C_2), 51.09 (C_9), 62.12 (C_3), 100.12 (C_6), 111.99 ($C_{12, 14, 16}$), 118.89 ($C_{13, 15}$), 143.77 (C_{11}), 157.31 (C_7), 179.39 (C_{10}), 190.95 (C_4). Figure (1).

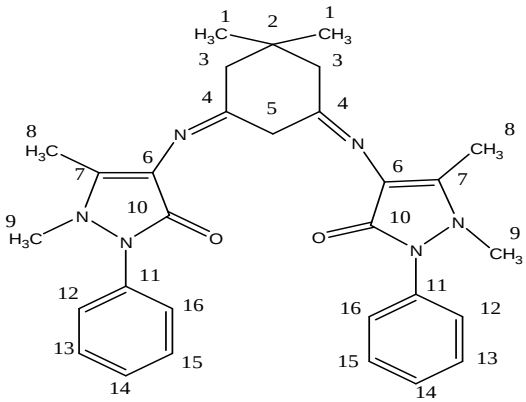

Fig (1) Structure of ligand

Preparation of Complexes:

The preparation of all complexes is essentially the same and so a generic description will be presented. To a solution of (L) (1mmole) in ethanol was added slowly to a solution of metal salt [$MnCl_2.4H_2O$ =0.197g;

$FeCl_3.6H_2O$ =0.27g; $CoCl_2.6H_2O$ =0.237g; $NiCl_2.6H_2O$ =0.237g; $CuCl_2.2H_2O$ =0.17g; $ReCl_5$ =0.363g; $H_2PtCl_4.6H_2O$ =0.446g] (1mmol) in (ethanol and water) ratio (1:1) with stirring the mixture was refluxed for (3hrs). The solid was collected by filtration recrystallized from methanol dried at room temperature. Elemental analysis data color and yield for the complexes are given in Table (1).

Programs used in theoretical calculation:

Hyper Chem-8 program is a sophisticated molecular modeler, editor and powerful computational package, that is known for its quality, flexibility and ease of use. It is also uniting 3D visualization and animation with quantum chemical calculations, molecular mechanics and dynamics. In the present work, parameterization method (PM3) was use for the calculation of heat of formation and binding energy for all metal complexes. PM3 is more popular than other semi-empirical method due to the availability of algorithms and it is more accurate than other method[5]. PM3 / TM is an extension of the PM3 method to include orbital's with transition metals. It is parameterized primarily for organic molecules and selected transition metals.

Microbiological investigations

For these investigations the filter paper disc method was applied according to[6]. The investigated isolates of bacteria were seeded in tubes with nutrient broth (NB). The seeded NB (1 cm^3) was homogenized in tubes with 9 cm^3 of melted (45 °C) nutrient agar (NA). The homogeneous suspensions were poured into Petri dishes. The discs of filter paper (diameter 4 mm) were ranged on the cool medium. After cooling on the formed solid medium, 2×10^{-5} dm^3 of the investigated compounds were applied using a micropipette. After incubation for 24 h in a thermostat at 25–27 °C, the inhibition (sterile) zone diameters (including disc) were measured and expressed in mm. An inhibition zone diameter over 7 mm indicates that the tested compound is active against the bacteria under investigation. The antibacterial activities of the

Results and Discussion:

The physical analytical data of (L) and its metal complexes are given in Table (1), which in a satisfactory agreement with the calculated values. The suggested molecular formulae also supported by subsequent spectral and molar ratio, magnetic moment and conductivity measurements. For the wide studied rang of molar concentration (10^{-5}-10^{-3}M) of the mixed solutions, only concentration of (10^{-4}M) obey Lambert-Beer's Law and showed intense color. A calibration curve was plotted on absorbance against molar concentration in the range (1×10^{-4}-3×10^{-4} M). Best fit straight lines were obtained Figure (2) with correlation factor R. > 0.998. The composition of the complexes formed in solution has been established by mole ration and job method. In both cases the results reveals (1:1) metal to ligand ratio.

Table (1) Analytical and physical data of the ligand and its complexes

Compounds	Formula M. wt	Color	M. P. °C	Yield %	Elemental analysis, found (Calc.)%				
					C	H	N	M	Cl
L	$C_{30}H_{34}N_6O_2$ 510	Deep yellow	219-220	87	70.56 (71.66)	6.71 (7.17)	16.46 (15.40)		
CoL	$C_{30}H_{34}N_6O_2Cl_2Co$ 640.47	Violate	265	74	56.26 (55.46)	5.35 (6.53)	13.12 (14.14)	9.20 (10.11)	11.07 (10.09)
NiL	$C_{30}H_{34}N_6Cl_2Ni$ 640.23	Yellow greenish	240	70	56.28 (55.82)	5.35 (4.53)	13.13 (14.14)	9.17 (11.00)	11.08 (9.98)
CuL	$C_{30}H_{34}N_6O_2Cl_2Cu$ 645	Deep Brown	266	75	55.86 (57.11)	5.31 (4.46)	13.03 (14.14)	9.85 (11.11)	10.99 (10.16)
PdL	$C_{30}H_{34}N_6PdCl_2$ 687.96	Brown	217 d	59	52.38 (53.40)	4.98 (3.80)	12.22 (14.14)	15.47 (16.86)	10.31 (11.41)
MnL	$C_{30}H_{34}N_6O_2MnCl_2$ 636.47	Brown	228 d	68	56.61 (55.56)	5.38 (6.65)	13.20 (14.62)	8.63 (9.77)	11.41 (12.16)
$Fe^{III}L$	$C_{30}H_{34}N_6O_2FeCl_3$ 672.83	Red Brown	265 d	74	53.55 (54.54)	5.09 (4.90)	12.49 (13.88)	8.30 (9.88)	15.81 (16.77)
$Pt^{(IV)}L$	$C_{30}H_{34}N_6O_2PtCl_4$ 847.52	Red Brown	301 d	77	42.51 (43.02)	4.04 (4.14)	9.92 (10.11)	23.02 (22.87)	16.73 (15.99)
$Re^{v}L$	$C_{30}H_{34}N_6O_2ReCl_5$ 874.10	Brown	310 d	71	41.22 (42.02)	3.92 (4.01)	9.61 (10.11)	-	20.28 (21.08)

d=decompose

Infrared spectral studies of the ligand and its complexes

The IR spectrum of the ligand shows characterization bonds at (1728-1692) and (1640-1600) cm^{-1} due to the υ(C=O) and υ(C=N) functional groups, respectively[6,7]. The IR spectra of the complexes exhibited ligand bands with the appropriate shift due to complex formation Table (2). The υ(C=O) and υ(C=N) at (1728-1692) and (1640-1600) cm^{-1} in the free ligand shift to (1669-1714) and (1576-1610) cm^{-1}, respectively for the complexes. The reduction in bond order, upon complexation can be attributed to delocalization of metal electron density (t_2g) to the T_1- system of the ligand. These shifts confirm the coordination of the ligand via the oxygen and nitrogen of carbonyl and the azomethine groups to metal ions. At lower frequency the complexes exhibited bands around (590-508), (485-412) and (365-312) cm^{-1} assigned to the υ(M-N), υ(M-O) and υ(M-Cl), respectively[8,9].

Table (2) FTIR spectral data (wave number υ$^-$) cm^{-1} for the ligand and its complexes

Compound	C-H arom	C-Halip	C=O	C=N	M-N	M-O	M-Cl
L	3125 3080	2958 2926	1728 1692	1640 1600	-	-	-
MnL	3112 3045	2998 2919	1700 1688	1578	570 508	440	356
CoL	3012 3006	2937 2933	1697 1678	1610 1590	580 530	450 421	365
NiL	3110 3009	2940 2912	1708 1682	1621 1590	590 557	460 444	375
FeL	3117 3006	2937 2921	1705 1680	1576	577	439 420	320
CuL	3120 3060	2935	1711 1680	1612 1581	580 545	470 417	317
PdL	3118	2959 2939	1700	1620 1578	590 530	412	-
PtL	3120 3035	2944	1714 1669	1617 1571	590 572	485	318
ReL	3111 3035	2939	1712 1681	1612 1582	588	450 433	340 312

Mass spectrum

The electron impact spectrum of ligand (L) confirms the probable formula by showing a peak at (510m/z) cores bonding to Schiff base moiety [($C_{30}H_{34}N_6O_2$) calculated atomic mass 510]. The series of peak at 327 m/z is attributed to ($C_{18}H_{23}N_4O_2$) and 326 m/z is attributed to ($C_{18}H_{22}N_4O_2$). The fragmentation pattern is shown in Table (3).

Table (3) the fragmentation pattern for complexes of LC-Mass in units (m/z)

Complexes	Peak	Assignment
Pd Complex	687m/z	[$C_{30}H_{34}N_6Cl_2O_2Pd$]
	428m/z	[$C_{19}H_{22}N_4OPd$]
	259m/z	[$C_{11}H_{12}N_2Cl_2O$]
Cu Complex	645m/z	[$C_{30}H_{34}N_6Cl_2O_2Cu$]
	380m/z	[$C_{19}H_{23}Cl_2N_3O$]
	265m/z	[$C_{11}H_{11}CuN_3O$]
Ni Complex	640m/z	[$C_{30}H_{34}N_6O_2Ni$]
	569m/z	[$C_{30}H_{34}N_6Cl_2O_2Ni$]
Mn Complex	636m/z	[$C_{30}H_{34}N_6O_2MnCl_2$]
	342m/z	[$C_{11}H_{12}N_3O_2MnCl_2$]
	184m/z	[$C_{11}H_{10}N_3$]
	110m/z	[C_8H_{14}]
Re Complex	874m/z	[$C_{30}H_{34}N_6O_2ReCl_5$]
	472m/z	[$C_{11}H_9N_3O_2ReCl_2$]
	402m/z	[$C_{19}H_{25}Cl_3N_3$]

Electronic spectral, magnetic moments, and conductivity measurements

The electronic spectrum at the ligand exhibits intense absorption at (282,330) and 348 nm attributed to $\pi \rightarrow \pi^*$ and $n \rightarrow \pi^*$, respectively.

The magnetic moment value 3.872B.M. at Co(II) complex is typical for distorted octahedral geometry[10]. The electronic spectrum for this complex showed three broad peaks at 15432, 20000 and 25000cm^{-1} assigned to $^4T_1g \rightarrow {}^4T_1g_F$, $^4T_1g \rightarrow {}^4T_1g_P$ and $^4T_1g \rightarrow {}^4A_2g_F$ transition, respectively[11]. The Ni(II) complex exhibits peaks at 20408 and 15384cm^{-1} which assign to $^3A_2g \rightarrow {}^3T_1g_{(P)}$ and $^3A_2g \rightarrow {}^3T_1g_{(F)}$ transition, respectively suggesting an octahedral geometry around the Ni(II) ion [12]. The magnetic moment value at this complex consistent with octahedral geometry structure. The spectra of the Cu(II), Mn(II), Fe(III), Pt(IV) and Re(V) complexes of together with the Mett value Table(4) suggest octahedral geometry around for complexes. The spectrum of Pd(II) complex gave two bands peak at 20325 and 12658cm^{-1} assigned to $^1A_1g \rightarrow {}^1B_1g$ and $^1A_1g \rightarrow {}^1A_2g$ transition, respectively suggesting an square planar geometry[13-15]. The molar conductivity value of the complexes were consistent with non-electrolytes 2:1 electrolytes for Pd(II) and Pt(IV) complexes, 1:1 electrolytes for Fe(III) complex and 3:1 electrolytes Re(V) complex. See for the scheme of the preparation ligand and complexes Figure (3).

Table (4) Electronic data and molar conductivity for the metal complexes

Complexes	Molar Conductive cm^2 s mole^{-1}in DMSO	μ_{eff} M. B.	λ_{max} nm	˜υcm^{-1}	Assignment
CoL Octahedral	27	3.872	280 346 400 500 648	35714 29801 25000 20000 15432	Ligand Field C. T $^4T_1g(F) \rightarrow {}^4A_2g$ F $^4T_1g(F) \rightarrow {}^4T_1g$ P $^4T_1g(F) \rightarrow {}^4T_1g$ F
NiL Octahedral	23	2828	289 346 394 490 650	34602 28901 25380 20408 15384	Ligand Field C. T $^3A_{2g\ F} \rightarrow {}^3T_1g$ (p) $^3A_{2g\ F} \rightarrow {}^3T_1g$ (F) $^3A_{2g\ F} \rightarrow {}^3T_2g$ (F)
CuL Octahedral	19	1.732	436 385 590	28901 25974 16949	Ligand Field C. T $^2Eg \rightarrow {}^2T_2g$ (D)
PdL Square planer	147	Diamagnetic	380 410 492 790	26315 24390 20325 12658	Ligand Field C. T $^1A_1g \rightarrow {}^1B_1g$ $^1A_1g \rightarrow {}^1A_2g$
MnL Octahedral	19	1.05	344 368 505	29669 271714 19802	Ligand Field C. T $^6A_1g \rightarrow {}^4T_1g$ (G) $^6A_1g \rightarrow {}^4T_1g$ (D)
$Fe^{III}L$ Octahedral	83	5.77	344 371 640	29069 26954 21739	Ligand Field C. T $^5T_2g \rightarrow {}^5Eg$ (D)
PtL Octahedral	155	Diamagnetic	389 587 892	640 100 68	$\pi \rightarrow \pi^*$ $^1A_1g \rightarrow {}^1T_2g\ \nu_2$ $^1A_1g \rightarrow {}^1T_1g\ \nu_1$
ReL Octahedral	217	1.05	344 368 492 790	29669 271714 203 126	Ligand Field C. T $^6A_1g \rightarrow {}^4T_1g$ (G) $^6A_1g \rightarrow {}^4T_1g$ (D)

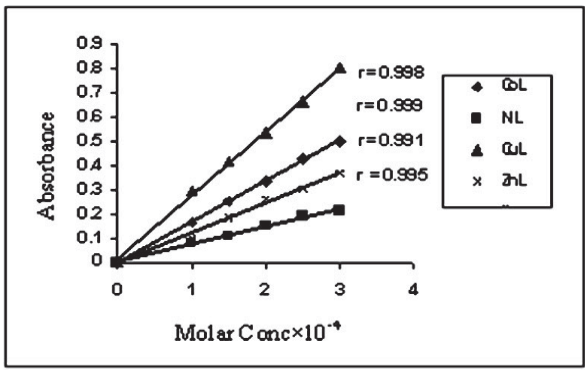

Fig (2) Linear Relation between Molar Concentration and Absorbance

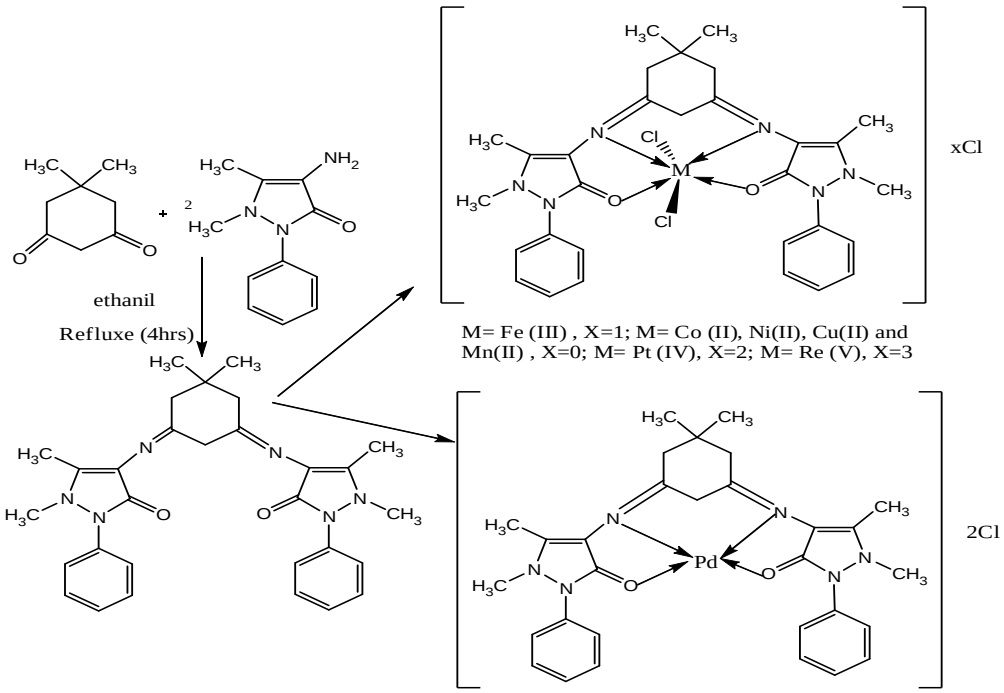

Fig (3) scheme of the preparation ligand and complexes

Thermal analyses TGA

The results of thermo gravimetric analyses of L and complexes are given in Table (5). The thermograms have been carried out in the range of 25–700 °C at a heating rate of 10 °C/min in nitrogen atmosphere, they showed an agreement in weight loss between their results obtained from the thermal decomposition and the calculated values, which supports the results of elemental analysis and confirms the suggested formulae. Thus, the ligand L showed a common general behavior as the first step ($C_{18}H_{11}N_2O_2$) was loss of $C_{12}H_{23}N_4$ moiety followed by the other parts of the ligand L. Furthermore, the final step of the thermolysis reactions of the complexes was found to give the metal oxide (L) = $C_{30}H_{34}N_6O_2$ [101.892% Found (99.999% Cal) (130-390 °C) → $C_{18}H_{11}N_2O_2$ [56.28% Found (56.274% Cal)] (390-697 °C) → $C_{12}H_{23}N_4$ [45.614% Found (43.725%Cal).

1-$C_{30}H_{34}N_6O_2Cl_3Fe$ (672.83) (35–190 °C) → $C_{11}H_{12}N_2OCl_3$ [42.89% Found (43.80% Cal)].

2-$C_{19}H_{22}N_4OFe$ (378.3) (190-690 °C) → $C_{19}H_{22}N_4$ [44.78% Found (45.54% Cal)].

3-FeO^+ [12.33% Found (10.67% Cal)]. Total wt. loss = 87.67% Found (89.34% Cal) and final residue: 12.33% Found (10.66% Cal).

1-$C_{30}H_{34}N_6O_2Cl_2Co$ (640.47) (25-200 °C) → Cl_2 [12.21% Found (11.08% Cal)].

2-$C_{30}H_{34}N_6O_2Co$ (569.56) (200-700 °C) → $C_{30}H_{34}N_6O$ [76.43% Found (77.13% Cal)].

3-CoO [11.36% Found (11.79% Cal)]. Total wt. loss = 88.64% Found (88.21% Cal) and final residue: 11.36% Found (11.79% Cal).

1-$C_{30}H_{34}N_6O_2Cl_2Ni$ (640.23) (25-200 °C) → Cl_2 [12.11% Found (11.08% Cal)].

2-$C_{30}H_{34}N_6O_2Ni$ (569.56) (200-700 °C) → $C_{30}H_{34}N_6O$ [76.53% Found (77.10% Cal)].

3-NiO [11.36% Found (11.82% Cal)]. Total wt. loss = 88.64% Found (88.18% Cal) and final residue: 11.36% Found (11.82% Cal).

1-$C_{30}H_{34}N_6O_2Cl_2Pd$ (687.96) (30-390 °C) → $C_{11}H_8N_3Cl_2$ [35.97% Found (36.77% Cal)].

2-$C_{19}H_{26}N_3O_2Pd$ (617.05) (390-690 °C) → $C_{30}H_{34}N_6O$ [45.52% Found (44.91% Cal)].

3-PdO [18.51% Found (18.82% Cal)]. Total wt. loss = 81.49% Found (81.68% Cal) and final residue: 18.51% Found (18.32% Cal).

1-$C_{30}H_{34}N_6O_2Cl_2Cu$ (645.08) (30-195 °C) → $C_6H_6Cl_2$ [22.87% Found (23.09% Cal)].

2-$C_{24}H_{28}N_6O_2Cu$ (496.08) (195-695 °C) → $C_{24}H_{28}N_6O$ [65.75% Found (64.48% Cal)].

3-CuO [11.38% Found (12.43% Cal)]. Total wt. loss = 88.62% Found (87.57% Cal) and final residue: 11.38% Found (12.43% Cal).

1-$C_{30}H_{34}N_6O_2Cl_2Mn$ (636.47) (35-400 °C) → $C_6H_6Cl_2$ [22.07% Found (23.41% Cal)].

2-$C_{24}H_{28}N_6O_2Mn$ (487.47) (400-700 °C) → $C_{24}H_{28}N_6O$ [65.75% Found (65.36% Cal)].

3-MnO [12.18% Found (11.23% Cal)]. Total wt. loss = 87.82% Found (88.77% Cal) and final residue: 12.18% Found (11.23% Cal).

1-$C_{30}H_{34}N_6O_2Cl_4Pt$ (847.52) (35-400 °C) → $C_6H_6Cl_4$ [26.87% Found (25.95% Cal)].

2-$C_{24}H_{28}N_6O_2Pt$ (627.52) (400-700 °C) → $C_{24}H_{28}N_6O$ [46.87% Found (47.19% Cal)].

3-CuO [26.26% Found (26.86% Cal)]. Total wt. loss = 73.74% Found (73.14% Cal) and final residue: 26.26% Found (26.86% Cal).

1-$C_{30}H_{34}N_6O_2Cl_5$ Re (874.1) (35-150 °C) → $C_6H_6Cl_5$ [28.87% Found (29.23% Cal)].

2-$C_{24}H_{28}N_6O_2Re$ (618.6) (150-430 °C) → C_6H_5N [9.87% Found (10.41% Cal)].

3-$C_{18}H_{23}N_5O_2Re$ (527.6) (430-700 °C) → $C_{18}H_{23}N_5$ [36.87% Found (35.35% Cal)].

4-ReO_2 [24.39% Found (25.01% Cal)]. Total wt. loss = 75.61% Found (74.99% Cal) and final residue: 24.39% Found (25.01% Cal).

Table 5 Thermodynamic data of the thermal decomposition of ligand and their complexes.

Sam (step	T range (°C)	n	R^2	Tmax (K)	Ea (kJ mol^{-1})	ΔH* (kJ mol^{-1})	A (sec^{-1} $\times 10^{7}$)	ΔS* (J mol^{-1} K^{-1})	ΔG* (kJ mol^{-1})	K $\times 10^{-7}$
L =1	130-390	1	0.995	570.64	10.160737	5.70751	3.661	-104.996	61.946	9.095102
L=2	390-697	1	0.998	877.36	13.851965	13.1808	7.791	-102.075	95.086	6.45457
PtL=1	35-400	0.9	0.989	547.79	5.71848	1.16415	5.84729	-101.293	56.6514	0.39608
PtL=2	400-700	0.9	0.997	848.51	13.25878	6.20427	9.76425	-100.668	91.6221	0.228822
MnL1	35-400	0.9	0.989	545.79	5.57028	1.03258	6.16336	-100.824	56.0618	0.430953
MnL=2	400-700	0.9	0.997	849.51	12.43878	5.37596	0.75906	-121.9189	108.947	1.9989
FeL=1	35-190	0.9	0.996	409.65	6.187388	2.78155	16.6018	-90.196	39.7168	0.858326
FeL=2	190-690	0.9	0.988	846.74	11.866	4.82622	12.4259	-98.646	88.353	0.35427
CuL=1	30-195	0.9	0.996	409.77	6.27826	2.87143	2.0264	-107.691	47	0.10174
CuL=2	195-695	0.9	0.988	847.74	11.866	4.81792	12.5302	-98.58648	88.393	0.35752
NiL=1	30-375	0.9	0.99	545.79	5.57031	1.0326	6.17163	-100.8137	56.055	0.43153
NiL=2	375-700	0.9	0.996	850.51	11.602	4.53087	13.7918	-97.5911	87.533	0.420629
CoL=1	25-200	0.9	0.997	409.77	6.289644	2.88339	2.02715	-107.688	47.0031	0.101652
CoL=2	200-700	0.9	0.989	846.74	11.69165	4.65185	13.0333	-98.24933	87.8435	0.38090
PdL=1	30-390	0.9	0.99	546.19	5.989	1.448	5.07571	-102.445	57.4027	0.32368
PdL=2	390-690	0.9	0.997	852.51	12.6143	5.5265	2.8008	-111.0917	100.233	7.21642
ReL=1	35-150	0.9	0.997	345.18	5.96778	3.09795	1.53783	-108.5589	40.5703	7.25169
ReL=2	150-430	0.9	0.993	632.54	9.1435	3.8845	5.42426	-103.1137	69.1081	0.19629
ReL=3	430-700	0.9	0.997	750.06	14.46375	8.22775	6.5654	-102.943	85.4412	0.112099

Kinetic studies

Coats–Redfern is the method mentioned in the literature related to decomposition kinetics studies; this method is applied in this study[16]. From the TG curves, the activation energy, E, pre-exponential factor, A, entropy, ΔS, enthalpy, ΔH, and Gibbs free energy, ΔG were calculated by the Coats–Redfern method where: ΔH= E - RT and ΔG= ΔH - TΔS. Kinetic parameters are calculated by employing the Coats– Redfern equations, are summarized in Table (5). The Coats– Redfern equation may be written as the following:

$$log\left[\frac{1-(1-\alpha)^{1-n}}{T^2(1-n)}\right] = log\frac{ZR}{qE}\left[1-\frac{2RT}{E}\right] - \frac{E}{2.303RT} \quad n\neq 1 \text{ for complex} \qquad (1)$$

$$log\left[\frac{-log(1-\alpha)}{T^2}\right] = log\left[\frac{AR}{\beta E}(1-\frac{2RT}{E}\right]\frac{E}{2.303RT} \quad n\neq 1 \text{ for ligands} \qquad (2)$$

Where α is the mass loss at the completion of the reaction, R is the gas constant, Ea is the activation energy in J mol^{-1} and q is the heating rate. Since *1–2 RT/Ea ≈ = 1*, a plot of the left-hand side of the above equation against and ΔE* was calculated from the slope and A (Arrhenius constant) was found from the intercept. The activation entropy ΔS*, the activation enthalpy ΔH* and the free energy of activation ΔG* were calculated using the following equations:

$$S^* = 2:303(logAh/KT)R; H^* = E^* - RT; G^* = H^* - T_S S^* \cdots 3$$

Where K and h are the Boltzmann's and Planck's constants, respectively. The calculated values of ΔE*, ΔS*, ΔH* and ΔG* for the dehydration and the decomposition steps are given in Table (5). The activation energies of the decomposition were found to be in the range of 134–208 J mol^{-1}.According to the kinetic data obtained from TGA

curves, the negative values of activation entropies ΔS* indicate more ordered activated complexes than the reactants and the reaction is slow[17].

Theoretical study

The vibration spectra Schiff base L were calculated by using a semi-empirical PM3 method. The results obtained for wave numbers are presented in Table (6), and the comparison with the experimental values indicates some deviations. These deviations may be due to the harmonic oscillator approximation and lack of electron correlation. It was reported [18] that frequencies coupled with Hartree- Fock Theory (HFT) approximation and quantum harmonic oscillator approximations tend to be 10% too high.

Optimized geometries' energy of metal complexes for ligand

Theoretical probable structures of metal complexes with ligand were calculated to search for the most probable model building stable structure, these shapes, show the calculated optima geometries for ligand and their metal complexes as shown in Figure (4). The results of PM3 method of calculation in the gas phase for binding energies and heat of formation of complexes are described in Table (6). The comparison of experimental and theoretical vibration frequencies is tabulated in Table (7).

Electrostatic potential (E.P)

Electron distribution governs the electrostatic potential of molecules and describes the interaction of energy of the molecular system with a positive point charge, so it is useful to find sites of reaction in a molecular positive charged species that tend to attack a molecule where the E.P. is strongly negative electrophilic attach[19]. The E.P of free ligand was calculated and plotted as 3D contour to investigate the reactive sites of the molecules, and one can interpret the stereochemistry and rates of many reactive involving soft electrophiles and nucleophiles in terms of the properties of frontier orbital's (HOMO and LUMO). Overlap between the HOMO and LUMO values was plotted as 3D contour to get more information about these molecules. The results of calculation showed that the LUMO of transition metal ion prefers to react with the HOMO of nitrogen atoms of ligand as shown in Figure (5).

Table (5) Conformation energies in (kJ mol^{-1}) for the ligand and complexes

Comp.	PM3		Comp.	PM3	
	ΔH_f°	ΔE_b		ΔH_f°	ΔE_b
L	1928.2795993	-3995.5384007	PdL	2136.4264527	-3877.3915473
MnL	88.4979704	-7397.4150296	FeL	210.8897177	-6927.125282
CoL	121.4043223	-7376.5386777	NiL	3450.3750690	-2634.2229310
CuL	265.543243	-4675.322179	ReL	132.76576297	-7652.546235
PtL	123.314242	-6543.646497			

Table (6) Comparison of experimental and theoretical vibration frequencies for ligand and complexes

Compound	C=O	C=N	M-N	M-O	M-Cl
L	*1728 *1692 ** 1726 **1700 ***0	*1640 *1600 **1650 **1603 ***0	-	-	-
MnL	*1700 *1688 **1702 **1691 ***0	*1578 **1571 ***0	*570 *508 **582 ** 500 ***0	*440 ** 445 ***0	*356 **360 ***0
CoL	*1697 *1678 **1700 **1670 ***0	*1610 *1590 ** 1600 **1601 ***0	*580 *530 **578 **533 ***0	*450 *421 **444 **420 ***0	*365 **362 ***0
NiL	*1708 *1682 **1703 **1681 ***0	*1621 *1590 **1624 **1591 ***0	*590 *557 **591 **555 ***0	*460 *444 **466 **442 ***0	*375 **377 ***0
FeL	*1705 *1680 **1702 **1681 ***0	*1576 **1573 ***0	*577 **578 ***0	*439 *420 **433 ***0	*320 **321 ***0
CuL	*1711 *1680 **1710 **1677 ***0	*1612 *1581 **1610 **1580 ***0	*580 *545 **581 **544 ***0	*470 *417 **476 **420 ***0	*317 **312 ***0
PdL	*1700 **1703 ***0	*1620 *1578 **1611 **1580 ***0	*590 *530 **591 **533 ***0	*412 **410 ***)	-
PtL	*1714 *1669 **1715 **1672 ***0	*1617 *1571 **1616 **1574 ***0	*590 *572 **600 **571 ***0	*485 **488 ***0	*318 **321 ***0
ReL	*1712 *1681 **1710 **1682 ***0	*1612 *1582 **1611 **1581 ***0	*588 **589 ***0	*450 *433 **451 **431 ***0	*340 *312 **344 **311 ***0

*Experimental frequency. ** Theoretical frequency. *** Error% due to main difference in the experimental measurements and theoretical treatments of vibration spectrum.

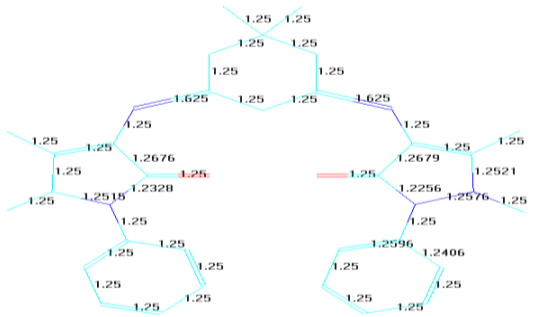

length of the bonds ligand

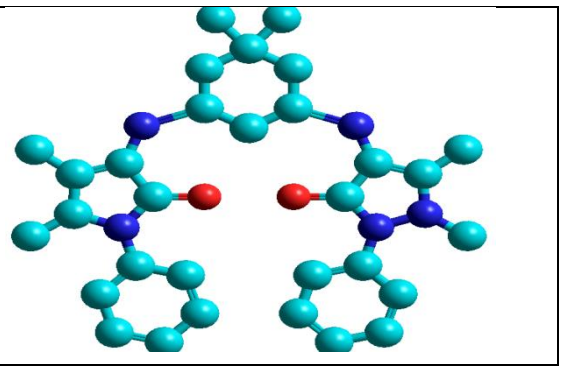

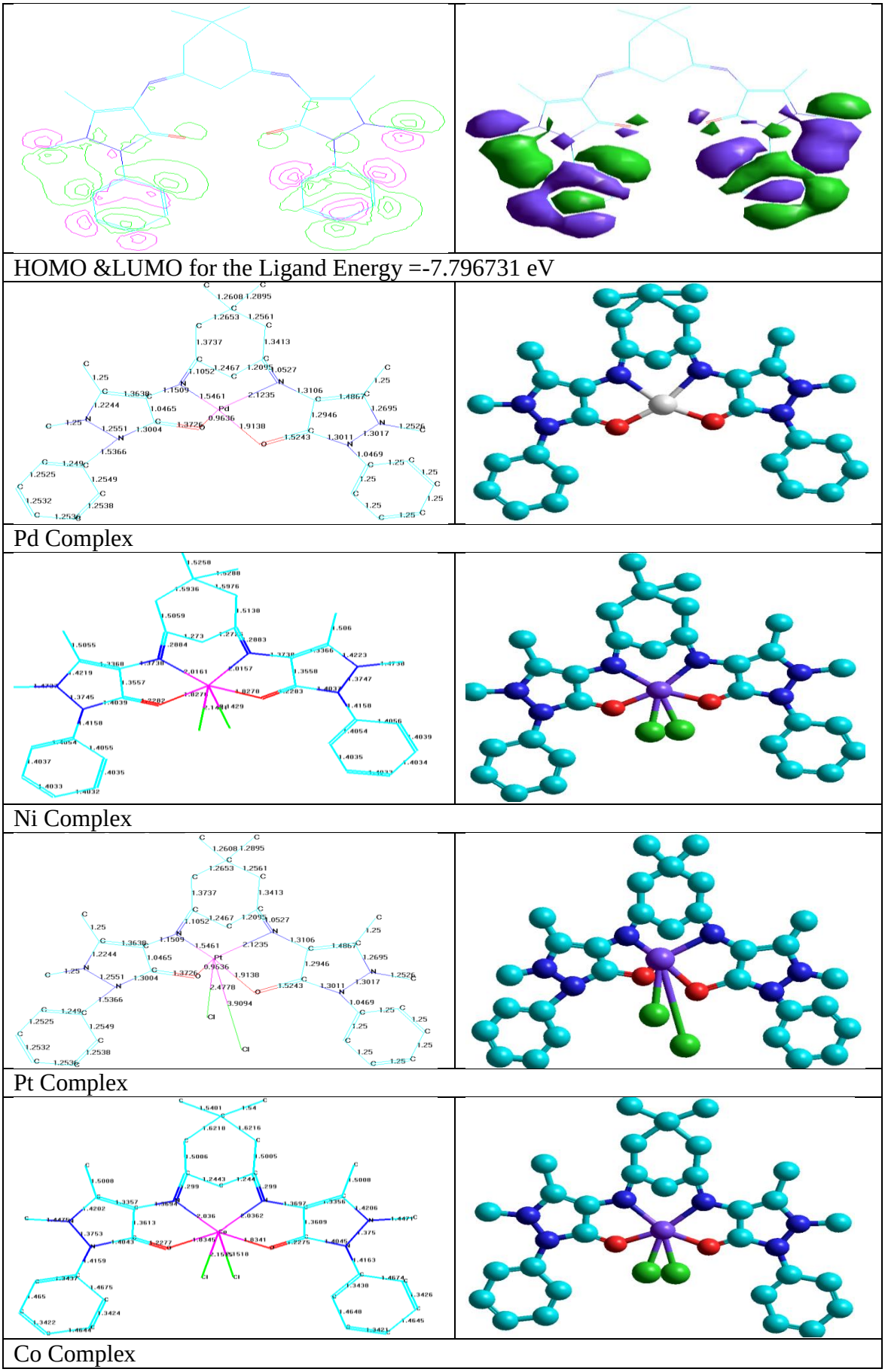

Fig (4) Conformational structure of ligand and their complexes.

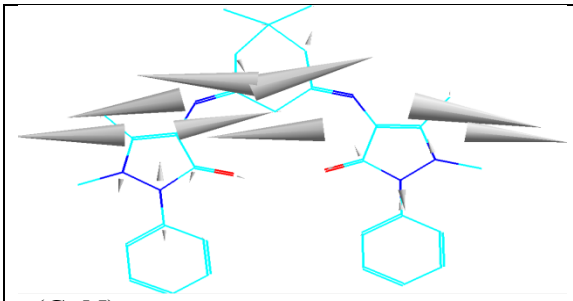

υ(C=N)

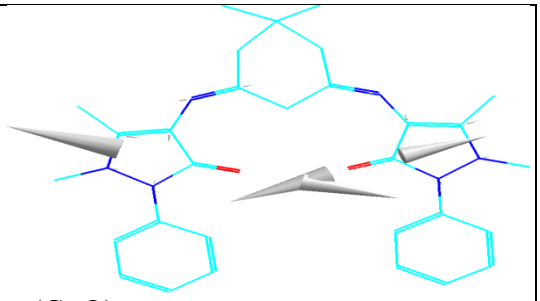

υ (C=O)

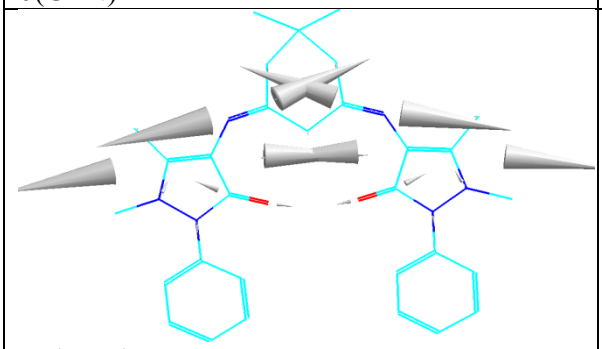

υ (C=N)

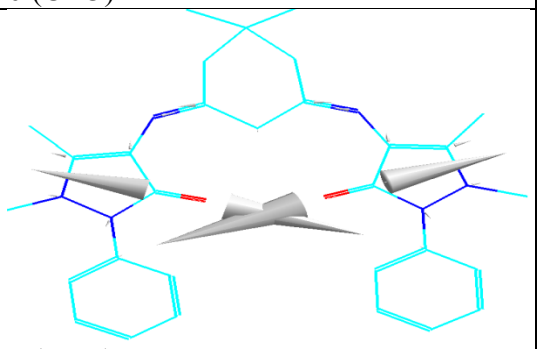

υ (C=O)

For ligand

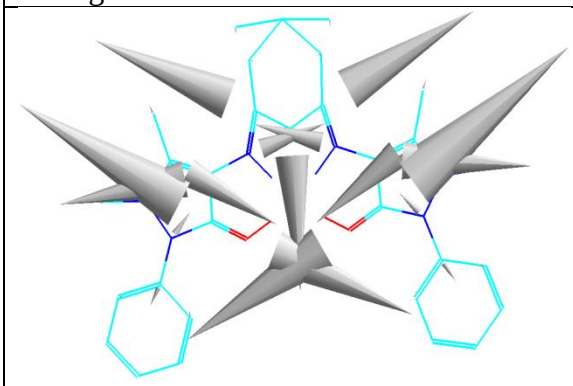

υ (C=O)

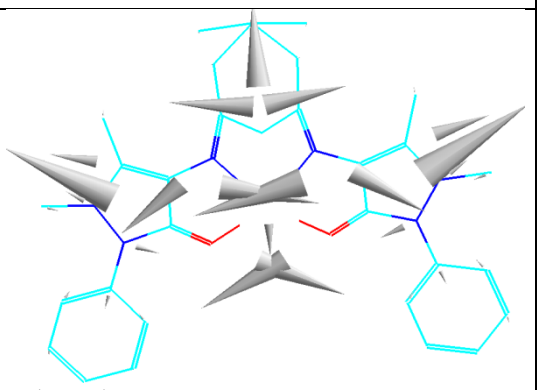

υ (C=N)

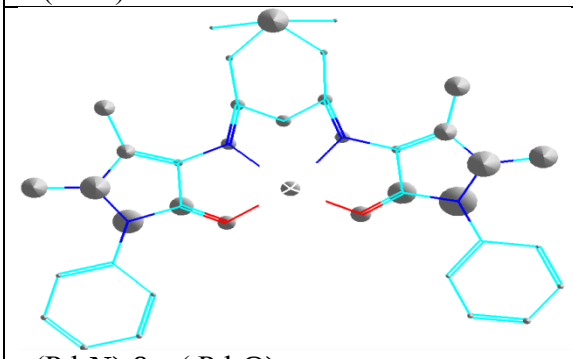

υ(Pd-N) & υ(Pd-O)

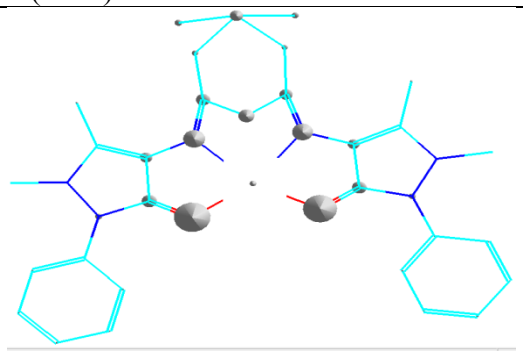

υ(Pd-N) & υ(Pd-O)

For Pd Complex

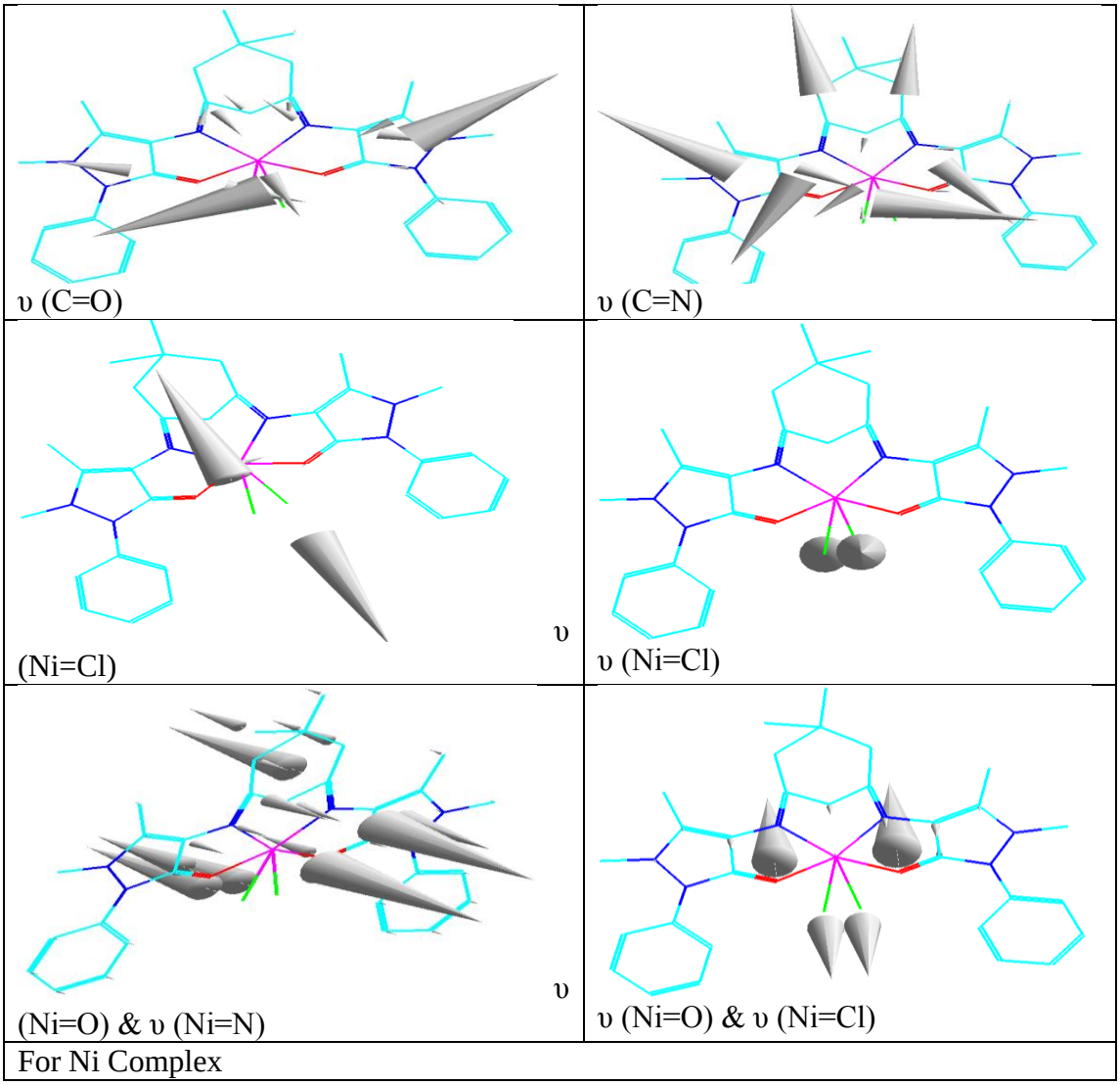

Fig (5) the calculated vibrational frequencies ligand and its complexes.

Microbiological investigation

The biological activity of ligand and their metal complexes was tested against bacteria; we used more than one test organism to increase the chance of detecting antibiotic principles in tested materials. The organisms used in the present investigation included two Gram positive bacteria (*B. subtilis and S. aureus*) and two Gram negative bacteria (*E. coli and P. aeruginosa*). The results of the bactericidal screening of the synthesized compounds are recorded in Table (7). An influence of the central ion of the complexes in the antibacterial activity against the tested Gram positive and Gram negative organisms shows that the complexes have an enhanced activity compared to the ligand itself.

Table (7) Antibacterial activity data of ligands and their complexes as inhibition zone (mm).

Compound	*Bacillus subtilis G+*	*Staphylococcus aureus G+*	*Escherichia coli G⁻*	*Pseudomonas aeruginosa G⁻*
L	18	16	19	18
MnL	22	21	23	16
CoL	20	21	24	21
NiL	15	23	21	22
FeL	18	23	22	20
CuL	20	22	19	26
PdL	21	16	18	19
PtL	22	22	19	24
ReL	21	22	23	24

Key to interpretation: Less than 10 mm=inactive, 10– 15 mm=weakly active, 15–20 mm=moderately active, more than 20 mm= highly active.

References:

1. Anitha, C. Sheela, C. D. Tharmaraj, P. and Sumathi, S. 2012. Spectroscopic studies and biological evaluation of some transition metal complexes of azo Schiff-base ligand derived from (1-phenyl-2,3-dimethyl-4-aminopyrazol-5-one) and 5-((4-chlorophenyl)diazenyl)-2-hydroxybenzaldehyde, Spectrochimica Acta Part A: Mole. and Biomolec. Spec., 96: 493-500.
2. Gupta, T. Patra, A. Dhar, K. S. Nethaji, M. and Chakravarty,A. R. 2005.Synthesis, Characterization and Antiamoebic Activity of Benzimidazole Derivatives and Their Vanadium and Molybdenum Complexes, J. Chem Sci. 117(12):12-18.
3. Samir,A. Abd El-Halim, H. F. Abd El-sadek,M.S. Yahia,I.S. and Wahab,L.A.2012.Synthesis, thermal characterization, and antimicrobial activity of lanthanum, cerium, and thorium complexes of amino acid Schiff base ligand. J Therm Anal Calorim, 109(1): 671-681.

4- Foresman, J. C. and Frisch, C. 1996. Exploring Chemistry with Electronic Structure Methods, second ed. Gaussian Inc., Springer, Berlin.

5- EL-Wahed,M. G. Refat, M. S. and El-Megharbel, S.M. 2009. Spectroscopic, thermal and biological studies of coordination compounds of sulfasalazine drug: Mn(II), Hg(II), Cr(III), ZrO(II), VO(II) and Y(III) transition metal complexes. Indian Academy of Sciences, Bull. Mater. Sci. 32(2): 205-214.

6- Raman, N. Johnson, S. Joseph, J. Sakthivel, A. and Dhaveethu, J. 2008. Synthesis and Characterization of Zno Microcrstal Tubes"., J. Chil. Chem. Soc. 53(3):1599-1604.

7- Abbas, A. S. and Shaimaa A. Sh. 2011. Synthesis, characterization, Stuctural Studies and Biological Activity of aNew Schiff Base –Azo Ligand and its Complexation with Selected Metal Ions, Oriental J. Chem. 27(3): 825-845.

8- Shaimaa,A.Sh. Yang,F. and Abbas, A.S. 2009. Synthesis and Characterization of Mixed Ligand Complexes of 8-Hydroxyquinoline and o-hydroxybenzylidene-1-phenyl-2,3-dimethyl-4-amino-3-pyrazolin-5-on with Fe(II), Co(II), Ni(II) and Cu(II) ions, European J. Scie. Resea, 33(4):702-709.

9- Nakamoto N. 2009. “Infrared and Raman Spectra of Inorganic and Coordination Compounds", 6th Ed, Part 2 John wiley and Sons, Inc., New Jersy.

10- Sliverstein R. M. and Webser X. F. 2005. “Spectrometric Identification of Organic Compounds”. 7th Ed., Jon Wiley and Son, Inc. USA.

11- Lever, A.B.P. 1968. Inorganic Electronic Spectroscopy .New York.6.121.

12- Abbas, A.S. 2013. Metal Complexes of Multidentate Schiff Base-Azo Ligand: Synthesis, Characterization and Biological Activity, Dirasat, Pure Scie. , 39 (1): 61-72.

13- Shaker, Sh. A. 2010. Preparation and Spectral Properties of Mixed-Ligand Complexes of VO(II), Ni(II), Zn(II), Pd(II), Cd(II) and Pb(II) with Dimethylglyoxime and N-Acetylglycine, E-J. Chem , 7 (4): 1598-1604.

14- Alhadi, A. A. Shaker, Sh. A. Yehye, W. A. Ali, H. M. and Abdullah, M. A. 2012. Synthesis magnetic and spectroscopic studies of Ni(II), Cu(II), Zn(II) and Cd(II) Complexes of a newly Schiff bas derived from 5-bromo-2-(hydroxybezylidene)-3,4,5-(trihydroxybenzohydrzide), Bull. Chem. Soc. Ethiop, 26 (1): 95-101.

15- Coats, A. W. and Redfern, J. P.1964. Kinetic parameters from thermogravimetric data. Nature, 201: 68–9.
16- Frost, A. A. and Pearson, R. G. 1964. Kinetics and Mechanism. 2nd ed., with permission of john wiley & sons, Inc Wiley, New York.
17- Anderson, W. P.; Behm, P. and Glennon, T. M. 1997. Searching the Conformational Space of Cyclic Molecules: A Molecular Mechanics and Density Functional Theory Study of 9-Crown-3, J. Phys. Chem. A101:1920-1926.
18- Shaimaa. R. B. 2012. Synthesis, Spectral study and biological activity of some metal ions complexes with bidentate ligands, J. AL-Nahra. Uni. Sci. 15(3):30-42.

تحضير، تشخيص، تحلل حراري ودراسة تركيبية لمعقدات جديدة مع ليكاند رباعي السن

عباس علي صالح الحمداني **سحر صبيح حسن**

قسم الكيمياء- كلية العلوم للبنات- جامعة بغداد – بغداد - العراق

الخلاصة:

حضرت بعض معقدات الليكاند 4-(5-(1،5_ثنائي مثل -3-اوكسو-2-فنيل بايرازولدين-4-ايل ايمين)-3،3-ثنائي مثل سايكلو هكسيل ثنائي ايمين امينو)- 1، 5 – ثنائي مثل -2- فنيل -1- بايرازول -3 (2 هيدروجين) – اون الجديدة المحضرة مع كل المنغنيز الثنائي، الحديد الثلاثي، الكوبلت الثنائي، النيكل الثنائي ، النحاس الثنائي ، البلاديوم الثنائي ، الرينيوم الخماسي والبلاتين الرباعي . شخصت معقدات الليكاند المحضرة بالطرق الطيفية والتقنية الكيميائية والفيزيائية . القيم الطيفية اقترحت ان الليكاند رباعي السن له القابلية على التناسق مع الايونات الفلزية عن طريق ذرتي النتروجين وذرتي الاوكسجين . الدراسات بينت ان الاشكال الهندسية ثمانية السطوح فقط وبالنسبة الى البلاديوم كان الشكل الهندسي له مربع مستوي. اوجدت الثوابت الثرموديناميكية لكل من طاقة التنشيط ،طاقة جبس، الانتروبي ، الانثالبية وثابت الاستقرارية للمعقدات ككل بتقنية التحلل الحراري با ستعمال معادلة كوست – ريد فيرن كما درست المركبات المحضرة نظريا باستخدام برنامج الهايبر كيم الثامن لتحديد الاشكال الهندسية الاكثر استقراراً للمركبات بالحالة الغازية وتحديد حرارة التكوين وطاقة الترابط بدرجة الحرارة المطلقة لليكاند بالحالة الحرة والمعقدات بطريقة PM3 كما اجريت دراسة الفعالية البيولوجية للمركبات المحضرة ضد البكتريا *(Bacillus subtilis and Staphylococcus aureus)* (*Escherichia coli and Pseudomonas aeruginosa*).

الكلمات المفتاحية: قواعد شف ليكندات رباعية السن ، تحاليل حرارية، الثوابت الترموديناميكية الحركية.